

Understanding spin parity of $P_c(4450)$ and $Y(4274)$ in a hadronic molecular state picture

Jun He*

Department of Physics and Institute of Theoretical Physics,
Nanjing Normal University, Nanjing, Jiangsu 210097, China

Nuclear Theory Group, Institute of Modern Physics, Chinese Academy of Sciences, Lanzhou 730000, China and
Research Center for Hadron and CSR Physics, Lanzhou University and Institute of Modern Physics of CAS, Lanzhou 730000, China

The hidden-charmed pentaquark $P_c(4450)$ and the charmonium-like state $Y(4274)$ are investigated as a $\bar{D}^*\Sigma_c$ and a $D_s\bar{D}_{s0}(2317)$ molecular state, respectively. The spin parities of these two states cannot be well understood if only S-wave $\bar{D}^*\Sigma_c$ and $D_s\bar{D}_{s0}(2317)$ interactions are considered. In this work, the interactions are studied in a quasipotential Bethe-Salpeter equation approach with a partial wave decomposition on spin parity J^P , and the contributions of different partial waves are studied in a two-channel scattering model including a generating channel and an observation channel. Two poles at $4447 \pm 4i$ and $4392 \pm 46i$ MeV are produced from the $\bar{D}^*\Sigma_c$ interaction coupled with the $J/\psi p$ channel in $3/2^-$ wave and $5/2^+$ wave, respectively. The peak for the $5/2^+$ state has a comparable height as that of the $3/2^-$ state in the $J/\psi p$ invariant mass spectrum. The $D_s\bar{D}_{s0}(2317)$ interaction coupled with the $J/\psi\phi$ channel is studied and a pole at $4275 \pm 11i$ MeV is produced in $J^P = 1^+$ wave, which corresponds to P-wave $D_s\bar{D}_{s0}(2317)$ interaction. The pole from S-wave $D_s\bar{D}_{s0}(2317)$ interaction is far below that from P-wave interaction even the $J/\psi\phi$ threshold, so cannot be observed in the $J/\psi\phi$ channel. The result suggests that in these cases a state carrying a spin parity corresponding to P-wave interaction should be taken as seriously as these carrying a spin parity corresponding to S-wave interaction in the hadronic molecular state picture.

PACS numbers: 14.20.Pt, 03.65.Nk, 11.10.St

I. INTRODUCTION

The hadronic molecular state picture is one of the most popular interpretations of the exotic state in market [1]. It has been widely applied to explain a series of experimentally observed exotic states, which cannot be assigned in the conventional quark model but is close to the threshold of two hadrons. In the literature, people often focus on the bound state from S-wave interaction and assume the P-wave bound state should be difficult to form from hadron-hadron interaction and to observe in experiment. For example, the $X(3872)$ and the $Z_c(3900)$ are related to isoscalar and isovector S-wave $D\bar{D}^*$ states [2–4], and the $Y(4274)$ and the $Y(4140)$ are related to S-wave $D_s\bar{D}_{s0}(2317)$ and $D_s^{*+}D_s^{*-}$ states, respectively [5–8]. There also exist predictions of hidden-charmed pentaquark from S-wave anticharmed meson and charmed baryon interactions [9, 10].

The recent observation of the $P_c(4450)$ and $P_c(4380)$ at LHCb confirmed the existence of the hidden-charmed pentaquark. With the help of partial wave analysis, LHCb provides the information about spin parities as well as masses of these states [11–13]. Surprisingly, different from the predictions in Refs. [9, 10] the hidden-charmed pentaquarks $P_c(4380)$ and $P_c(4450)$ carry opposite parities. It is difficult to explain both states as hadronic molecular states from relevant S-wave anticharmed meson and charmed baryon interactions, i.e., $\bar{D}\Sigma_c^*$, $\bar{D}^*\Sigma_c$, and $\bar{D}^*\Sigma_c^*$ interactions. In Ref. [14], the authors proposed that the $P_c(4450)$ can be reproduced from S-wave interaction of a proton and a P-wave charmonium χ_{c1} , with a small coupling to the $J/\psi p$ channel. It is an interesting

interpretation but a little different from the standard molecular state picture because the attraction is from transition between the $\chi_{c1}p$ and $J/\psi p$ channel instead of the direct $\chi_{c1}p$ interaction which is suppressed according to the OZI rule. In Ref. [15], the $\bar{D}\Sigma_c^*$, $\bar{D}^*\Sigma_c$, and $\bar{D}^*\Sigma_c^*$ interactions were investigated in a quasipotential Bethe-Salpeter equation approach with a partial wave decomposition based on J^P . In such an approach, the orbital angular momentum L is not considered explicitly because it is not a good quantum number when the calculation is relativistic and the experimental result is provided with spin parity J^P directly. A bound state in $5/2^+$ wave is produced from the $\bar{D}^*\Sigma_c$ interaction, which can be explained as experimentally observed $P_c(4450)$ [15]. Such spin parity cannot be produced from S-wave interaction of a \bar{D}^* with 1^- and a Σ_c with $1/2^+$. So this bound state with $5/2^+$ should be from P- and F-wave $\bar{D}^*\Sigma_c$ interaction. Such a challenge also happens in the case of the $Y(4274)$. The spin parity 1^{++} determined at LHCb [12, 13] conflicts with previous S-wave $D_s\bar{D}_{s0}(2317)$ molecular state interpretation [5, 7], which suggests P-wave interaction should be also introduced in this case.

In this work we will study the $P_c(4450)$ and $Y(4274)$ in a quasipotential Bethe-Salpeter equation with a partial wave decomposition on spin parity J^P . The spin parity which corresponds to P wave will be considered and focused. In the literature, there are some studies about the P-wave molecular state [15–17], especially Ref. [17] where S-wave interaction is forbidden. However, explicit comparison of the effects of P wave and S wave on experimental observables, such as cross section and invariant mass spectrum, is scarce. Hence, in this work, we will focus on three questions:

- Admittedly, P-wave interaction should be weaker than S-wave interaction. We will study whether P-wave interaction is too weak to form a bound state, or weak but

* junhe@impcas.ac.cn

still enough to form a bound state in some cases.

- Can the P-wave bound state, if it can be produced, be observed as these from S-wave interaction?
- If the observed state corresponds to the P-wave bound state, it should be answered where is the S-wave bound state which should be easier to produce.

In the next section, the formalism adopted in the quasipotential Bethe-Salpeter equation approach is presented, and a toy model of two-channel scattering of scalar mesons is adopted to compare P-wave and S-wave contributions. In Sec. III, the LHCb pentaquarks $P_c(4450)$ and $P_c(4380)$ are studied as the $\bar{D}^*\Sigma_c$ molecular states. The $D_s\bar{D}_{s0}(2317)$ interaction and the $Y(4274)$ are studied in Sec. IV. The discussion and summary are given in the last section.

II. FORMALISM

In this work, we will introduce a two-channel scattering, which includes a generating channel and an observation channel, to study the relative magnitude of contributions of different spin-parity partial waves.

- Generating channel: It has a higher threshold and is adopted to generate the bound state by exchange of light mesons. In the cases considered in this work, the $\bar{D}^*\Sigma_c$ channel and the $D_s\bar{D}_{s0}(2317)$ channel are considered for the $P_c(4450)$ and the $Y(4274)$, respectively.
- Observation channel: It has a lower threshold and is adopted to observe the bound state generated by the generating channel. For the observation channels considered in this work, i.e. the $J/\psi p$ channel and the $J/\psi\phi$ channel, the interaction is very weak according to the OZI rule.

The generating and observation channels are coupled by exchanges of heavy mesons, D or D^* mesons here. With the transition between two channels, the bound state generated by the generating channel will leave the real axis in the complex plane and exhibit itself as a peak in the invariant mass spectrum of the observation channel. The contributions of different spin-parity partial waves in the observation channel can be compared. To study the two-channel scattering, a coupled-channel quasipotential Bethe-Salpeter equation approach will be adopted.

A. Quasipotential Bethe-Salpeter equation

The general form of the Bethe-Salpeter equation for the scattering amplitude reads

$$\begin{aligned} \mathcal{M}^{mn}(k'_1 k'_2, k_1 k_2; P) \\ = \mathcal{V}^{mn}(k'_1 k'_2, k_1 k_2; P) + \sum_l \int \frac{d^4 k''}{(2\pi)^4} \end{aligned}$$

$$\cdot \mathcal{V}^{ml}(k'_1 k'_2, k''_1 k''_2; P) G^l(k''_1 k''_2) \mathcal{M}^{ln}(k''_1 k''_2, k_1 k_2; P), \quad (1)$$

where \mathcal{V} is the potential kernel and G is the product of the propagators for two constituent particles. Here the momentum of the system $P = k_1 + k_2 = k'_1 + k'_2$, and the relative momentum $k'' = (k''_2 - k''_1)/2$. The superscript l, m or n remarks the different channels, generating and observation channel here.

The Bethe-Salpeter equation is usually reduced to a three-dimensional equation with a quasipotential approximation. To study the behavior of the one-boson-exchange interaction below threshold, the off-shellness of two constituent hadrons should be kept. Here we adopt a most economic method, that is, the covariant spectator theory [18, 19], which was explained explicitly in the appendices of Ref. [4] and applied to study the $\Lambda(1405)$, the $Z_c(4430)$, the $N(1875)$, and the $Z(3900)$ and the LHCb pentaquarks [4, 15, 20–23]. Written down in the center-of-mass frame where $P = (W, \mathbf{0})$, the propagator is

$$\begin{aligned} G &= 2\pi i \frac{\delta^+(k_2^2 - m_2^2)}{k_1^2 - m_1^2} \\ &= 2\pi i \frac{\delta^+(k_2^0 - E_2(\mathbf{p}))}{2E_2(\mathbf{p})[(W - E_2(\mathbf{p}))^2 - E_1^2(\mathbf{p})]}, \end{aligned} \quad (2)$$

where $k_1 = (k_1^0, -\mathbf{p}) = (W - E_2(\mathbf{p}), -\mathbf{p})$ and $k_2 = (k_2^0, \mathbf{p}) = (E_2(\mathbf{p}), \mathbf{p})$ with $E_{1,2}(\mathbf{p}) = \sqrt{M_{1,2}^2 + |\mathbf{p}|^2}$. A definition $G_0 = G/(2\pi i)$ will be used for convenience thereafter. The constituent particle 2, which is the heavier one, is put on shell to satisfy the charge-conjugation invariance because the meson-exchange model is adopted in the current work [24]. A numerical discussion about different choices of the oneshell constituent particle was made in Ref. [25], and no obvious differences were found with different choices. We would like to note that the covariance and the unitarity are kept in this quasipotential approximation.

After multiplying the polarized vector and spinor on both sides of Eq. (1), we obtain an equation for helicity amplitude as

$$\begin{aligned} i\mathcal{M}_{\lambda'\lambda}^{mn}(\mathbf{p}', \mathbf{p}) &= i\mathcal{V}_{\lambda'\lambda}^{mn}(\mathbf{p}', \mathbf{p}) + \sum_{l,\lambda''} \int \frac{d^3 \mathbf{p}''}{(2\pi)^3} \\ &\cdot i\mathcal{V}_{\lambda'\lambda''}^{ml}(\mathbf{p}', \mathbf{p}'') G_0^l(\mathbf{p}'') i\mathcal{M}_{\lambda''\lambda}^{ln}(\mathbf{p}'', \mathbf{p}), \end{aligned} \quad (3)$$

where \mathbf{p}, \mathbf{p}' and \mathbf{p}'' are the momenta of constituent 2. Here and hereafter, individual helicities are omitted where redundant and states are only labeled by the total helicities λ, λ' and λ'' .

In this work, we make a partial wave decomposition of the helicity amplitude \mathcal{M} based on spin parity J as [26]

$$\begin{aligned} \mathcal{M}_{\lambda'\lambda}(\mathbf{p}', \mathbf{p}) &= \sum_{J\lambda_R} \frac{2J+1}{4\pi} D_{\lambda_R\lambda'}^{J*}(\phi', \theta', 0) \\ &\cdot \mathcal{M}_{\lambda'\lambda,\lambda_R}^J(\mathbf{p}', \mathbf{p}) D_{\lambda_R\lambda}^J(\phi, \theta, 0), \end{aligned} \quad (4)$$

where $D_{\lambda_R\lambda}^J(\phi, \theta, 0)$ is the rotation matrix with J being the angular momentum for the partial wave considered and λ_R being

the helicity of the bound state. A definition $p \equiv |p|$ is adopted here in order to avoid confusion with the four-momentum p . Without loss of generality, we choose the scattering to be in the xz plane, the potential is written as

$$\mathcal{V}_{\lambda\lambda'}^J(p, p') = 2\pi \int d\cos\theta d_{\lambda\lambda'}^J(\theta_{p',p}) \mathcal{V}_{\lambda\lambda'}^J(p', p), \quad (5)$$

where the momenta $k_1 = (W - E, 0, 0, -p)$, $k_2 = (E, 0, 0, p)$ and $k'_1 = (W - E', -p' \sin\theta, 0, -p' \cos\theta)$, $k'_2 = (E', p' \sin\theta, 0, p' \cos\theta)$.

Besides the above partial wave decomposition, the amplitude with fixed parity is introduced as $\mathcal{M}_{\lambda\lambda'}^{J^P} = \mathcal{M}_{\lambda\lambda'}^J + \eta \mathcal{M}_{\lambda\lambda'}^{J-\lambda}$ with $\eta = PP_1P_2(-1)^{J-J_1-J_2}$, where P and $P_{1,2}$ are the parities and J and $J_{1,2}$ are the angular momenta for the system and particle 1 or 2 [29]. The partial wave Bethe-Salpeter equation with fixed spin parity J^P reads as [4]

$$i\hat{\mathcal{M}}_{\lambda\lambda'}^{mn,J^P}(p', p) = i\hat{\mathcal{V}}_{\lambda\lambda'}^{mn,J^P}(p', p) + \sum_{l,\lambda''} \int \frac{p''^2 dp''}{(2\pi)^3} \cdot i\hat{\mathcal{V}}_{\lambda\lambda''}^{ml,J^P}(p', p'') G^l(p'') i\hat{\mathcal{M}}_{\lambda''\lambda}^{ln,J^P}(p'', p), \quad (6)$$

where λ, λ' and $\lambda'' \geq 0$ and $\hat{\mathcal{M}}_{\lambda\lambda'}^{J^P} = f_{\lambda} f_{\lambda'} \mathcal{M}_{\lambda\lambda'}^{J^P}$, with $f_0 = \frac{1}{\sqrt{2}}$ and $f_{\lambda \neq 0} = 1$. The potential with fixed parity is of a form

$$\hat{\mathcal{V}}_{\lambda\lambda'}^{J^P}(p', p) = 2\pi f_{\lambda} f_{\lambda'} \int d\cos\theta [d_{\lambda\lambda'}^J(\theta_{p',p}) \mathcal{V}_{\lambda\lambda'}^J(p', p) + \eta d_{-\lambda\lambda'}^J(\theta_{p',p}) \mathcal{V}_{\lambda\lambda'}^J(p', p)]. \quad (7)$$

By using normalization of the Wigner D matrix, the integration of the amplitude is

$$\sum_{\lambda'\lambda} \int d\Omega |\mathcal{M}_{\lambda\lambda'}^J(p', p)|^2 = \sum_{J^P, \lambda' \geq 0, \lambda \geq 0} |\hat{\mathcal{M}}_{\lambda\lambda'}^{J^P}(p', p)|^2. \quad (8)$$

Since there is no interference between the contributions from different partial waves, total cross section or invariant mass spectrum can also be divided into partial-wave cross sections.

To solve the integral equation (6), we discretize the momenta p, p' , and p'' by the Gauss quadrature with a weight $w(p_i)$ and have [4]

$$M_{ik} = V_{ik} + \sum_{j=0}^N V_{ij} G_j M_{jk}. \quad (9)$$

The propagator G is of a form

$$G_{j>0} = \frac{w(p_j'') p_j''^2}{(2\pi)^3} G_0(p_j''),$$

$$G_{j=0} = -\frac{i p_0''}{32\pi^2 W} + \sum_j \left[\frac{w(p_j)}{(2\pi)^3} \frac{p_0''^2}{2W(p_j''^2 - p_0''^2)} \right], \quad (10)$$

with on-shell momentum

$$p_0'' = \frac{1}{2W} \sqrt{[W^2 - (M_1 + M_2)^2][W^2 - (M_1 - M_2)^2]}. \quad (11)$$

In this work, we will search for the pole of scattering amplitude as $M = (1 - VG)^{-1}V$. By analytic continuation into complex plane $W \rightarrow z$, the pole can be found by variation of z in the complex plane to satisfy $|1 - V(z)G(z)| = 0$.

B. Toy model: Two-channel scattering of scalar mesons

Since realistic interaction is complex, we present first a simple toy model to explain why we should not work with S-wave interaction only. Here, the generating channel is composed of two scalar particles with equivalent masses $M = 2.2$ GeV and observation channel is composed of two scalar particles with masses 1 and 3 GeV. All particles involved are assumed to be scalar and isoscalar particles for simplicity. In the current case, the 0^+ and 1^- waves with partial wave decomposition on spin parity J^P correspond to S and P waves, respectively.

The potential in the one-boson-exchange model for the two-channel scattering is written as,

$$i\mathcal{V} = \begin{pmatrix} \frac{C}{q^2 - m^2} & \frac{C'}{q^2 - m'^2} \\ \frac{C'}{q^2 - m'^2} & 0 \end{pmatrix}, \quad (12)$$

where q is momentum of exchanged meson. The C and C' describe the strengths of interactions for the generating channel and transition of two channels, respectively. In the cases of the $\bar{D}^*\Sigma - J/\psi p$ and $D_s \bar{D}_{s0}(2317) - J/\psi \phi$ interactions considered in the current work, the interaction in the generating channel is mediated by exchanges of light mesons, such as π and ρ mesons, and the coupling of generating and observation channel by exchanges of charmed mesons, such as the D meson. To connect with these realistic cases, in the toy model we choose $m = 0.5$ GeV and $m' = 2$ GeV, which are at the same order of masses of light meson and of charmed meson, respectively.

Before presenting the explicit numerical results about the S and P waves, we give a simple analytical discussion. According to the definition of partial-wave potential in Eq. (5), for a scalar system considered here the S-wave contribution is from the terms with $(\cos\theta)^0 = 1$, and the P-wave contribution is from the terms with $\cos\theta$ which usually appears with a factor of $\delta^2 = (p/M)^2$. If both constituents are on shell, we will have a very small δ because of the small binding energy of molecular state of an order of 10 MeV and large masses M of two constituent hadrons of the order of 1 GeV. It is why the suppression of the P-wave contribution seems obvious in the hadron physics community.

Now we take the potential of generating channel as an example to show why such an analysis is not so reliable for meson-exchange potential. If we assume δ small the potential can be written as

$$\frac{C}{q^2 - m^2} = \frac{C}{2M^2 - 2E_2(p) E_2'(p') + 2pp' \cos\theta - m^2}$$

$$\approx \frac{-C}{p^2 + p'^2 + m^2 - 2pp' \cos\theta}. \quad (13)$$

If the momentum $p^{(\prime)}$ is also much smaller than the mass of the exchanged meson m , the term $2pp' \cos\theta$ can be omitted so that the P-wave contribution vanishes. However, the exchanged meson is often light in the one-boson-exchange model. Furthermore, except at threshold it is impossible to put both constituent particles on shell. The momentum is not

fixed but a variable of integration in our quasipotential Bethe-Salpeter approach and popularly used Lippmann-Schwinger equation approach. It is often cut off at about 1 GeV, so the momentum may be larger than the mass of the exchanged meson.

In the chiral unitary approach, the cutoff in momentum can be seen as regularization [27], which can be related to the dimensional regularization as discussed in Ref. [28]. Inserting the potential in Eq. (12) into the partial-wave Bethe-Salpeter equation in Eq. (6), one can find that the convergence is not satisfied in our approach. Hence, a regularization is also needed in our approach. We will adopt an exponential regularization by introducing a form factor of exponential form in the propagator as

$$G_0(p) \rightarrow G_0(p)F(p) = G_0(p) \left[e^{-(k_1^2 - m_1^2)^2 / \Lambda^4} \right]^2, \quad (14)$$

with k_1 and m_1 being the momentum and mass of the charmed meson [4]. The particle 2 is not involved because of its on-shell-ness. With such regularization, the momentum usually spreads from 0 to about 1 GeV as presented in Fig. 1.

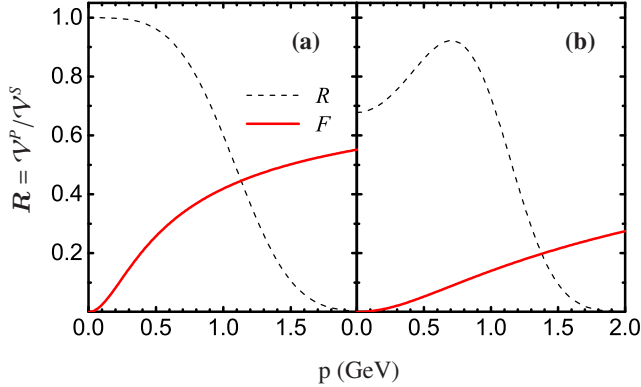


FIG. 1. (Color online) The ratio R between P-wave and S-wave potential. Part (a) is for the generating channel and Part (b) for the transition between the generating and the observation channel.

Here a binding energy $E = 10$ MeV is adopted and cutoff Λ is chosen at 2 GeV. For convenience, we plot the results with $p = p'$. The form factor $F(p)$ is about 50% at $p \approx 1$ GeV. So, it is unreliable to regard the P-wave contribution as a negligible contribution even for exchange of ρ , ω , σ or ϕ mesons, which is not so light as the π meson.

In Fig. 1, the ratio $R = \mathcal{V}^P/\mathcal{V}^S$ between the P-wave and S-wave potential with $p = p'$ is also depicted. It is obvious that the P-wave potential is smaller but of the same order of magnitude as the S-wave potential for exchange of a particle with mass $m = 0.5$ GeV. The ratio R for the transition of the generating and observation channel is smaller than that for the generating channel, which is due to larger mass of the exchanged meson.

The above analysis suggests that P-wave interaction is weaker than S-wave interaction but still promising to produce a bound state. In the following, we will make an explicit calculation to compare P-wave and S-wave contribution by taking explicit strengths $C = 6000$ GeV and $C' = 2000$ GeV as

an example. With potential in Eq. (12), the $\log|1 - V(z)G(z)|$ is plotted in Fig. 2 with variations of $\text{Re}(z)$ and $\text{Im}(z)$. The poles can be identified from the plot at z which satisfies $|1 - V(z)G(z)| = 0$. The square of the scattering amplitude for the observation channel

$$|\mathcal{M}_{obs}^{JP}|^2 = \sum_{\lambda' \geq 0, \lambda \geq 0} |\hat{\mathcal{M}}_{obs, \lambda' \lambda}^{JP}(p'_o, p_o)|^2, \quad (15)$$

which is the core of many observables, such as cross section and invariant mass spectrum, is also presented in Fig. 2. The scattering amplitudes $\hat{\mathcal{M}}_{obs, \lambda' \lambda}^{JP}(p'_o, p_o)$ correspond to the observation-channel part of amplitude $\hat{\mathcal{M}}_{\lambda' \lambda}^{JP}(p', p)$ with fixed spin parity in Eq. (8) with the momenta p' and p being chosen as on shell momentum defined in Eq. (11). The scattering amplitude is obtained by a numerical solution of the Bethe-Salpeter equation with fixed spin parity in Eq. (6) by transforming it to a matrix equation (9).

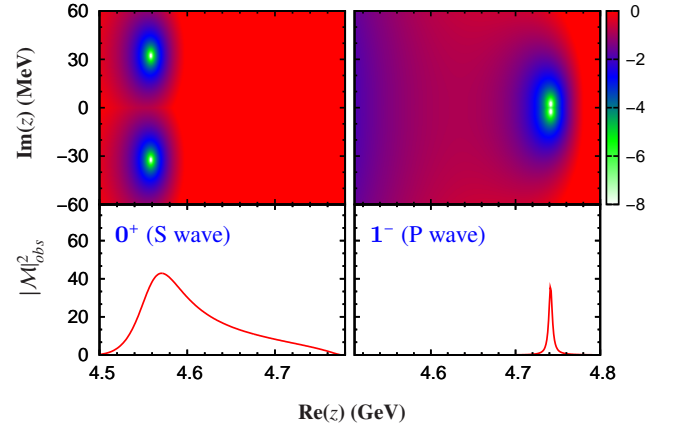


FIG. 2. The $\log|1 - V(z)G(z)|$ and square of scattering amplitude $|\mathcal{M}_{obs}^2$ for the toy model. The results in 0^+ (S wave) (left panel) and 1^- (P wave) (right panel) are drawn to the same scale.

A P-wave bound state is produced from the generation channel as well as a S-wave state. The P-wave state is closer to the threshold of the generating channel than the S-wave state, which is easy to understand because the P-wave interaction is, though strong enough to produce a bound state, but still weaker than the S-wave interaction. Such a phenomena will be helpful to answer where is S-wave bound state which should be easier to produce if the observed state corresponds to a P-wave bound state. It will be discussed later in the realistic case in the next section.

If only the generation channel is considered, the pole for the bound state is at the real axis. After transition of generating and observation channels is included, the poles for both S- and P-wave bound states leave the real axis to the complex plane. In other words, the transition will give the bound state width. In the model considered here, the S-wave and the P-wave states decay to the observation channel through S and P waves, respectively. The P-wave state has smaller width than the S-wave state because the transition between generating and observation channel in P wave is weaker than those

in S wave as shown in Fig. 1. However, such weakness in P wave has a relatively small affect on the height of peaks observed. The peak of the P-wave state observed in the observation channel is almost the same height as that of the S-wave state. Based on the results we concluded that the P-wave interaction is weaker but may be still enough to form an observable bound state, at least for the toy model considered here.

III. APPLICATION TO LHCb HIDDEN-CHARMED PENTAQUARKS

Now, we turn to a realistic case, the LHCb hidden-charmed pentaquarks. If these two pentaquarks are interpreted as the $\bar{D}\Sigma^*$ or $\bar{D}^*\Sigma$ molecular state, the opposite parities suggest that one of them is at least a P-wave state. Furthermore, the results in the toy model show that the P-wave state is narrower and closer to the threshold than the S-wave state, which has analogy to the narrower $P_c(4450)$ and wider $P_c(4380)$. Hence, the $P_c(4450)$ and $P_c(4380)$ may be a $5/2^+$ (P- and F-waves) state from the $\bar{D}^*\Sigma_c$ interaction, respectively. To confirm this assumption, a two-channel scattering will be constructed as the toy model.

For the generating channel $\bar{D}^*\Sigma_c$, an explicit discussion in the same quasipotential Bethe-Salpeter equation approach as the current work has been given in Ref. [15] with pseudoscalar (π , η), vector (ρ , ω) and scalar (σ) meson exchanges included. These two pentaquarks were observed in the $J/\psi p$ invariant mass spectrum, so we choose it as the observation channel. Since the $J/\psi p$ interaction is OZI suppressed, here we assume a potential $iV_{J/\psi\phi \rightarrow J/\psi\phi} = 0$ as in the toy model.

The transition between generating and observation channel is described by D and D^* exchanges. So we need the following Lagrangians [30–33]:

$$\begin{aligned}\mathcal{L}_{\Sigma_c ND^*} &= g_{\Sigma_c ND^*} \bar{N} \gamma_\mu \tau \cdot \Sigma_c D^{*\mu} + \text{H.c.}, \\ \mathcal{L}_{\Sigma_c ND} &= -ig_{\Sigma_c ND} \bar{N} \gamma_5 \tau \cdot \Sigma_c D + \text{H.c.}\end{aligned}\quad (16)$$

Based on SU(4) symmetry, the coupling constants $g_{\Sigma_c ND^*} = 3.0$, and $g_{\Sigma_c ND} = 2.69$ [30–32]. The coupling of heavy-light charmed mesons to J/ψ is of form [34–37]

$$\begin{aligned}\mathcal{L}_{D^* \bar{D} J/\psi} &= g_{D^* \bar{D} J/\psi} \epsilon_{\beta\mu\alpha\tau} \partial^\beta \psi^\mu (\bar{D}^* \overleftrightarrow{\partial}^\tau D^{*\alpha} + \bar{D}^{*\alpha} \overleftrightarrow{\partial}^\tau D) \\ \mathcal{L}_{D^* \bar{D} J/\psi} &= -ig_{D^* \bar{D} J/\psi} [\psi^\mu \bar{D}_\mu^* \overleftrightarrow{\partial}^\nu D_\nu^* - \psi^\mu \bar{D}^{*\nu} \overleftrightarrow{\partial}^\mu D_\nu^* \\ &\quad + \psi^\mu \bar{D}^{*\nu} \overleftrightarrow{\partial}^\nu D_\mu^*].\end{aligned}\quad (17)$$

The two couplings are related to a single parameter g_2 as $g_{D^* \bar{D}^* \psi} = 2g_2 \sqrt{m_\psi m_{D^*}}$, $g_{D^* D \psi} = 2g_2 \sqrt{m_D m_{D^*}/m_\psi}$ with $g_2 = \sqrt{m_\psi}/(2m_D f_\psi)$ and $f_\psi = 405$ MeV [34–37]. As discussed in Ref. [38], we do not consider the form factors for the light meson coupling with D^* and the $D^{(*)}$ coupling with J/ψ . A form factor as $f(q^2) = [\Lambda^2/(\Lambda^2 - q^2)]^2$, which satisfies the quark counting rule, is only introduced to the vertex for the baryon with a cutoff Λ which is chosen the same as the cutoff in the propagator for simplification.

The potential kernel can be obtained with the Lagrangians given above as our previous work in Ref. [15]. In our model, only one free parameter, the cutoff Λ , is involved, which will

be determined by comparison with experiment. As in the toy model, the poles of two-channel scattering in $3/2^-$ and $5/2^+$ waves are searched by variation of z in the complex plane to satisfy $|1 - V(z)G(z)| = 0$, and presented in Fig. 3. The $J/\psi p$ invariant mass spectrum of $\Lambda_b^0 \rightarrow J/\psi K^- p$ decay is given approximately as [39, 40]

$$\frac{d\sigma}{dW} = C |\mathcal{M}_{J/\psi p}^{J^P}|^2 \lambda^{\frac{1}{2}}(W^2, m_{J/\psi}^2, m_p^2) \lambda^{\frac{1}{2}}(\tilde{W}^2, W^2, m_{K^-}^2) / W, \quad (18)$$

with \tilde{W} being total energy of the decay process, that is, the mass of Λ_b^0 . The square of the $J/\psi p$ scattering amplitude $|\mathcal{M}_{J/\psi p}^{J^P}|^2$ is defined and calculated analogously to that in the toy model in Eq. (15).

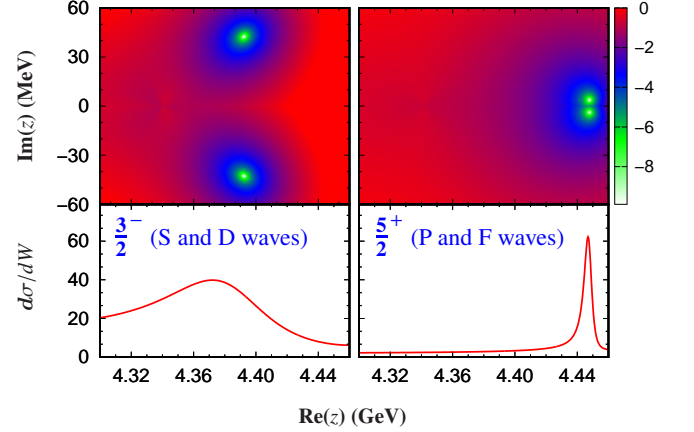


FIG. 3. The $\log |1 - V(z)G(z)|$ and the $J/\psi p$ mass spectrum for the $\bar{D}^*\Sigma_c$ interaction coupled with the $J/\psi p$ channel at cutoff $\Lambda=2$ GeV. The results in $\frac{3}{2}^-$ wave (left panel) and $\frac{5}{2}^+$ wave (right panel) are drawn to the same scale.

The cutoff Λ is varied to produce two poles which can be related to two LHCb pentaquarks. At cutoff $\Lambda = 1.7$ GeV, which is close to the cutoff in the nucleon-nucleon interaction [18, 19], a pole at $4447 \pm 4i$ MeV is found in $5/2^+$ -wave $\bar{D}^*\Sigma_c$ interaction. Correspondingly, a narrow peak appears in the $J/\psi p$ mass spectrum near the $\bar{D}^*\Sigma_c$ threshold. The small binding energy and width of this state is due to the relatively weak interaction in P and F waves. Obviously, this state can be identified as the experimentally observed $P_c(4450)$. In the $3/2^-$ wave corresponding to S and D waves, a pole at $4392 + 46i$ MeV is found, whose peak is rather broad and far from the $\bar{D}^*\Sigma_c$ threshold because of the relatively strong interaction in this partial wave. Hence, as in the toy model, the P-wave state is bound more loosely and narrower than the S-wave state, which is consistent with the experimental observations of the $P_c(4450)$ and the $P_c(4380)$ [11].

In Table I, more results of the position of the poles with variation of the cutoff are listed to show the sensitivity to the parameter, cutoff Λ . In this work we are more interested in the bound state in the $5/2^+$ wave near the $\bar{D}^*\Sigma_c$ threshold. The results show that the mass of this higher pole decreases by about 20 MeV with cutoff increasing from 1.6 to 1.8 GeV.

Empirically, it is reasonable to conclude that the result is not sensitive to the cutoff for the higher pole. The running of the lower pole in $\frac{3}{2}^-$ wave is faster than the higher pole. However, considering large experimental uncertainty of mass and width of this state, the result is not so sensitive to the cutoff.

TABLE I. The position of the poles from the $\bar{D}^*\Sigma_c - J/\psi p$ interaction with the variation of cutoff Λ . The higher and lower lines are for $J^P = \frac{5}{2}^+$ and $\frac{3}{2}^-$ waves, respectively. The cutoff Λ and position z are in units of GeV and MeV, respectively.

Λ	1.60	1.65	1.70	1.75	1.80
$\frac{5}{2}^+$	4456+i2	4451+i3	4447+i4	4443+i5	4438+i6
$\frac{3}{2}^-$	4441+i29	4415+i38	4392+i46	4370+i47	4350+i48

It is well known that a resonance leads to a rapid rotation of evolution of complex amplitude in the Argand diagram. The molecular state will show a circular trajectory near the position of the peak. In Fig. 4, the Argand diagram are shown with the energy region from 4.30 to 4.46 GeV as in Fig. 3. The energy region is divided into 500 parts, each of which is plotted as a dot in Fig. 4.

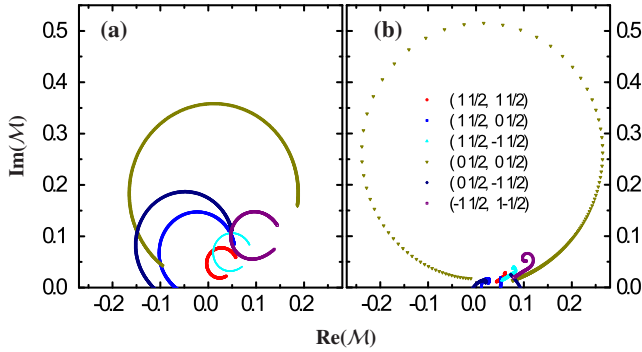


FIG. 4. (Color online) The Argand diagrams for the $\frac{3}{2}^-$ wave (panel a) and $\frac{5}{2}^+$ wave (panel b). The numbers in the legend are for the helicities $(\lambda_1\lambda_2, \lambda'_1\lambda'_2)$ of the helicity amplitudes.

All independent helicity amplitudes are presented and it is found that $M_{(01/2,01/2)}$ is the most important one. Because the amplitudes for the $J/\psi p$ scattering are adopted here, the results cannot be compared directly with the LHCb experiment [11]. But there is still something interesting observed. The molecular states really give a rapid rotation at energies near peaks as expected which is a behavior characteristic of a real resonance structure. For the $5/2^+$ state corresponding to $P_c(4450)$, almost an entire circle is formed while for the $3/2^-$ state corresponding to $P_c(4380)$ only an arc is formed. The analogous behaviors can be found in the Argand diagram of the LHCb experiment [11]. Almost all dots for the $3/2^-$ state are at the circle, which reflects the resonance structure cover all energy region from 4.30 to 4.46 GeV as shown in Fig. 3. But for the $5/2^+$ state, only a few dots are involved in the rapid

rotation, which reflects the small width of this state. The dots out of the resonance region assemble at the (0, 0) point, and do not show a circular trajectory.

IV. APPLICATION TO THE $Y(4274)$

In Refs. [5, 7], the $D_s D_{s0}(2317)$ interaction has been studied and the $Y(4274)$ is assigned as an S-wave $D_s D_{s0}(2317)$ molecular state with quantum number $J^{PC} = 0^{-+}$, which conflicts with recent LHCb experiments [12, 13]. To reproduce the LHCb spin parity of the $Y(4274)$ we need to introduce the P-wave interaction. Considering that the $D_s \bar{D}_{s0}(2317)$ interaction is mediated by ϕ and η exchanges, it is possibly strong enough to generate a P-wave bound state.

As in Ref. [7], the potential of the $D_s \bar{D}_{s0}(2317)$ interaction by light meson exchanges can be obtained with the Lagrangian from the heavy quark field theory [37],

$$\mathcal{L} = i \frac{-2h}{\sqrt{6}f_\pi} (D_s^\dagger \overleftrightarrow{\partial}^\mu D_{s0} + D_{s0}^\dagger \overleftrightarrow{\partial}^\mu D_s) \partial_\mu \eta - i \frac{\beta g_V}{\sqrt{2}} D_s^\dagger \overleftrightarrow{\partial}^\mu D_s \phi_\mu + i \frac{\beta' g_V}{\sqrt{2}} D_{s0}^\dagger \overleftrightarrow{\partial}^\mu D_{s0} \phi_\mu, \quad (19)$$

where the coupling constants $h = -0.56 \pm 0.28$, $\beta\beta' = 0.90$, $g_V = m_\rho/f_\pi = 5.8$ with $f_\pi = 132$ MeV [5, 6, 37, 41]. Since β and β' are not well determined in the literature, we choose $\beta\beta' = 0.9\eta_{\beta\beta'}$ and take $\eta_{\beta\beta'}$ as a free parameter.

Here we will use these potentials to study the 1^{++} (P-wave) bound state as well as the 0^{-+} (S-wave) bound state. To compare the contributions of S-wave and P-wave states in the $J/\psi\phi$ channel, we also introduce the transition between $D_s \bar{D}_{s0}(2317)$ and $J/\psi\phi$ channel through D_s^* exchange. Different from the toy model and the case of $P_c(4450)$ and $P_c(4380)$, the 1^{++} (P-wave) and 0^{-+} (S-wave) bound states from the $D_s \bar{D}_{s0}$ interaction decay into $J/\psi\phi$ in S and P waves, respectively. The Lagrangians for J/ψ coupling to $D_s^* \bar{D}_s$ and $D_s^* \bar{D}_{s0}(2317)$ reads [37, 42]

$$\begin{aligned} \mathcal{L}_{D_s^* \bar{D}_s J/\psi} &= 2g_2 \sqrt{\frac{m_{D_s} m_{D_s^*}}{m_\psi}} \epsilon_{\beta\mu\alpha\tau} \partial^\beta \psi^\mu \cdot (\bar{D}_s^\dagger \overleftrightarrow{\partial}^\tau D_s^{*\alpha} + \bar{D}_s^{*\alpha} \overleftrightarrow{\partial}^\tau D_s), \\ \mathcal{L}_{D_s^* \bar{D}_{s0} J/\psi} &= -2g_3 \sqrt{m_{D_s} m_{D_{s0}} m_\psi} \psi \cdot \bar{D}_s^* D_{s0} + \text{H.c.}, \end{aligned} \quad (20)$$

where $g_3 = \sqrt{m_\psi}/f_\psi$. The Lagrangians for J/ψ coupling to $D_s^* \bar{D}_s$ and $D_s^* \bar{D}_{s0}(2317)$ reads [37, 42],

$$\begin{aligned} \mathcal{L}_{D_s^* D_s \phi} &= -i \sqrt{2} \lambda g_V \epsilon_{\lambda\alpha\beta\mu} (D_s^{*\mu\dagger} \overleftrightarrow{\partial}^\lambda D_s + D_s^\dagger \overleftrightarrow{\partial}^\lambda D_s^{*\mu}) \partial^\alpha \phi_\beta, \\ \mathcal{L}_{D_s^* D_{s0} \phi} &= \sqrt{2} \varpi g_V (D_{s0}^\dagger \overleftrightarrow{\partial}^\alpha D_s^{*\beta} - D_s^{*\beta\dagger} \overleftrightarrow{\partial}^\alpha D_{s0}) (\partial_\alpha \phi_\beta - \partial_\beta \phi_\alpha) \\ &\quad - \sqrt{2} \zeta g_V \sqrt{m_{D_{s0}} m_{D_s^*}} (D_{s0}^\dagger D_s^{*\mu} + D_s^{*\mu\dagger} D_{s0}) \phi_\mu, \end{aligned} \quad (21)$$

where $\lambda = 0.56 \text{ GeV}^{-1}$, $\zeta = 0.727$ and $\varpi = 0.364$. As in the case of the pentaquark, we do not consider the form factors for the light meson coupling with D_s while form factor are introduced to the vertex for D_{s0}^* because it is an excited state. Since there does not exist experimental or theoretical

information about the form factor for D_{s0}^* meson. Form factor as $f(q^2) = \Lambda^2/(\Lambda^2 - q^2)$ are introduced to the vertex for the D_{s0}^* meson with a cutoff Λ which is chosen the same as the cutoff in the propagator for simplification.

It is found that with $\Lambda = 1.8$ GeV and $\eta_{\beta\beta^*} = 1.8$, a pole at $4275 + 11i$ MeV is produced from the $D_s\bar{D}_{s0}(2317)$ interaction with 1^{++} , which is presented in Fig. 5. As in the case of the toy model and the case of the $P_c(4450)$, the 1^{++} (P-wave) state appears near the threshold while a 0^{-+} (S-wave) state is far from the threshold of the generating channel. The pole near the threshold at $4275 \pm 11i$ MeV can be related to the $Y(4274)$ with the spin parity 1^{++} suggested by LHCb. It is interesting to find that the 0^{-+} (S-wave) state is below the J/ψ threshold, which explains why it cannot be observed in experiment.

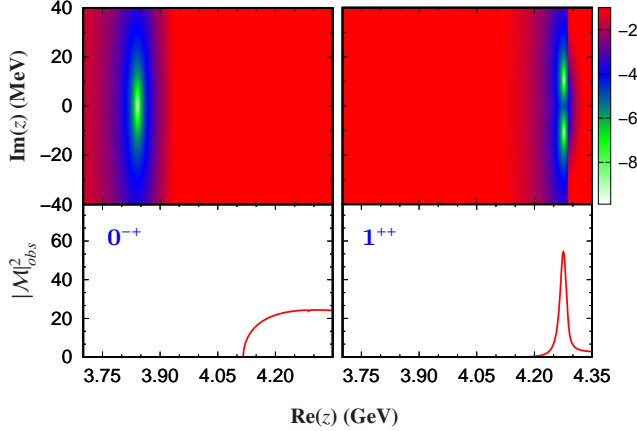


FIG. 5. The $\log|1 - V(z)G(z)|$ and the $J/\psi\phi$ mass spectrum for the $D_s\bar{D}_{s0}(2317)$ interaction coupled with the $J/\psi\phi$ channel at cutoff $\Lambda=2$ GeV. The results in 0^{-+} wave (left panel) and 1^{++} wave (right panel) are drawn to the same scale. The explicit partial waves on orbital angular momentum L are not given here because the 1^{++} (P-wave) and 0^{-+} (S-wave) bound states from the $D_s\bar{D}_{s0}(2317)$ interaction decay into $J/\psi\phi$ in S and P waves, respectively.

In Table II, more results about the position of the poles are listed as in the hidden-charmed pentaquark case. Analogously, the pole near the $D_s\bar{D}_{s0}(2317)$ threshold is not sensitive to cutoff. The mass decreases by about 10 MeV with cutoff increasing from 1.7 to 1.9 GeV. The running of the lower pole in the $\frac{3}{2}^-$ wave is faster than the higher pole.

TABLE II. The position of poles from the $D_s\bar{D}_{s0}(2317) - J/\psi\phi$ interaction with the variation of cutoff Λ . The higher and lower lines are for $J^P = 1^{++}$ and 0^{-+} waves, respectively. The cutoff Λ and position z are in units of GeV and MeV, respectively.

Λ	1.70	1.75	1.80	1.85	1.90
1^{++}	4278+i10	4276+i10	4275+i11	4272+i12	4269+i13
0^{-+}	3900	3872	3841	3809	3774

V. DISCUSSION AND CONCLUSION

In this work, we study the $\bar{D}^*\Sigma_c$ and $D_s\bar{D}_{s0}(2317)$ interactions and their relation to the experiment observed $P_c(4450)$ and $Y(4274)$ in the hadronic molecular state picture. The spin parities of these two states cannot be reproduced from only S-wave interactions, so the spin parties which correspond to P wave are considered in this work. A pole near the $\bar{D}^*\Sigma_c$ threshold and a pole near $D_s\bar{D}_{s0}$ threshold can be found with quantum number $5/2^+$ and 1^{++} , respectively. These two poles can be related to the experimentally observed $P_c(4450)$ and $Y(4274)$.

The bound states with spin parties which correspond to S wave are also produced as expected. When the P-wave state is produced near threshold, the S-wave state is far from the threshold. For the $\bar{D}^*\Sigma_c$ interaction, the pole from $3/2^-$ -wave interaction locates at about 4390 MeV, which can be related to the $P_c(4380)$ state. As suggested in Ref. [1] existence of two or more resonant signals around 4380 MeV, especially those with spin parity $3/2^-$, cannot be excluded because of the large widths for the $P_c(4380)$ obtained here and in experiment. For the $D_s\bar{D}_{s0}(2317)$ interaction, the S-wave state is far from the threshold even below the $J/\psi\phi$ threshold, so cannot be observed in experiment.

By introducing an observation channel, the effects of states in different partial waves on experiment observables are discussed. For the toy model and the $\bar{D}^*\Sigma_c - J/\psi p$ interaction, the P-wave state near threshold is narrower than the S-wave state far from the threshold, but the height of the peak of the former is of the same order of magnitude as the peak of the latter. In this work, only two channels are included. If the width of the P-wave state is really so smaller than S-wave state after all possible channels included, the P-wave state should be easy to observe in experiment. Back to the questions in the Introduction, at least for the cases considered in this work,

- P-wave interaction is weaker but may be still enough to form a bound state.
- The P-wave bound state can be observed as these from S-wave interaction.
- The S-wave bound state should be far from the threshold if the observed state corresponds to the P-wave bound state.

ACKNOWLEDGMENTS

This project is partially supported by the National Natural Science Foundation of China (Grants No. 11275235 and No.11675228), and the Major State Basic Research Development Program in China (No. 2014CB845405).

-
- [1] H. X. Chen, W. Chen, X. Liu and S. L. Zhu, Phys. Rept. **639**, 1 (2016)
 - [2] N. A. Tornqvist, Phys. Lett. B **590**, 209 (2004)
 - [3] F. E. Close and P. R. Page, Phys. Lett. B **578**, 119 (2004)
 - [4] J. He, Phys. Rev. D **92**, 034004 (2015)
 - [5] X. Liu, Z. G. Luo and S. L. Zhu, Phys. Lett. B **699**, 341 (2011) Erratum: [Phys. Lett. B **707**, 577 (2012)]
 - [6] J. He and X. Liu, Eur. Phys. J. C **72**, 1986 (2012)
 - [7] J. He and P. L. Lü, Nucl. Phys. A **919**, 1 (2013)
 - [8] X. Liu and S. L. Zhu, Phys. Rev. D **80**, 017502 (2009) Erratum: [Phys. Rev. D **85**, 019902(E) (2012)]
 - [9] J. J. Wu, R. Molina, E. Oset and B. S. Zou, Phys. Rev. Lett. **105**, 232001 (2010)
 - [10] Z. C. Yang, Z. F. Sun, J. He, X. Liu and S. L. Zhu, Chin. Phys. C **36**, 6 (2012)
 - [11] R. Aaij *et al.* [LHCb Collaboration], Phys. Rev. Lett. **115**, 072001 (2015)
 - [12] R. Aaij *et al.* [LHCb Collaboration], Phys. Rev. Lett. **118**, no. 2, 022003 (2017)
 - [13] R. Aaij *et al.* [LHCb Collaboration], Phys. Rev. D **95**, no. 1, 012002 (2017)
 - [14] U. G. Meissner and J. A. Oller, Phys. Lett. B **751**, 59 (2015)
 - [15] J. He, Phys. Lett. B **753**, 547 (2016)
 - [16] J. He, and X. Liu, Phys. Rev. D **82**, 114029 (2010)
 - [17] X. W. Kang and J. A. Oller, arXiv:1606.06665 [hep-ph].
 - [18] F. Gross, J. W. Van Orden and K. Holinde, Phys. Rev. C **45**, 2094 (1992).
 - [19] J. W. Van Orden, N. Devine and F. Gross, Phys. Rev. Lett. **75**, 4369 (1995).
 - [20] J. He, Phys. Rev. D **90**, 076008 (2014)
 - [21] J. He and P. L. Lü, Int. J. Mod. Phys. E **24**, 1550088 (2015)
 - [22] J. He and P. L. Lü, Chin. Phys. C **40**, 043101 (2016)
 - [23] J. He, Phys. Rev. C **91**, 018201 (2015)
 - [24] F. Gross, Few Body Syst. **30**, 21 (2001)
 - [25] J. He, “Nucleon resonances $N(1875)$ and $N(2100)$ as strange partners of LHCb pentaquarks,” arXiv:1701.03738 [hep-ph].
 - [26] S. U. Chung, Spin Formalisms, CERN 71-8 (2014)
 - [27] E. Oset and A. Ramos, Nucl. Phys. A **635**, 99 (1998)
 - [28] J. A. Oller, E. Oset and J. R. Pelaez, Phys. Rev. D **59**, 074001 (1999) Erratum: [Phys. Rev. D **60**, 099906 (1999)] Erratum: [Phys. Rev. D **75**, 099903 (2007)]
 - [29] G. Penner, Nucleon Resonance Analysis in a Coupled-Channel Approach, Ph.D thesis, Universität Giessen (2002)
 - [30] Y. Dong, A. Faessler, T. Gutsche and V. E. Lyubovitskij, Phys. Rev. D **81**, 014006 (2010)
 - [31] Q. F. L and Y. B. Dong, Phys. Rev. D **93**, no. 7, 074020 (2016)
 - [32] C. W. Shen, F. K. Guo, J. J. Xie and B. S. Zou, Nucl. Phys. A **954**, 393 (2016)
 - [33] E. J. Garzon and J. J. Xie, Phys. Rev. C **92**, no. 3, 035201 (2015)
 - [34] H. Y. Cheng, C. Y. Cheung, G. L. Lin, Y. C. Lin, T. M. Yan and H. L. Yu, Phys. Rev. D **47**, 1030 (1993)
 - [35] T. M. Yan, H. Y. Cheng, C. Y. Cheung, G. L. Lin, Y. C. Lin and H. L. Yu, Phys. Rev. D **46**, 1148 (1992) Erratum: [Phys. Rev. D **55**, 5851 (1997)].
 - [36] M. B. Wise, Phys. Rev. D **45**, 2188 (1992).
 - [37] R. Casalbuoni, A. Deandrea, N. Di Bartolomeo, R. Gatto, F. Feruglio and G. Nardulli, Phys. Rept. **281**, 145 (1997)
 - [38] P. L. Lü and J. He, Euro. Phys. J. A **52**, 359 (2016)
 - [39] T. Hyodo, A. Hosaka, E. Oset, A. Ramos and M. J. Vicente Vacas, Phys. Rev. C **68**, 065203 (2003)
 - [40] F. Aceti, M. Bayar, E. Oset, A. M. Torres, K. P. Khemchandani, J. M. Dias, F. S. Navarra and M. Nielsen, Phys. Rev. D **90**, 016003 (2014)
 - [41] C. Isola, M. Ladisa, G. Nardulli and P. Santorelli, Phys. Rev. D **68**, 114001 (2003)
 - [42] P. Colangelo, F. De Fazio and T. N. Pham, Phys. Rev. D **69**, 054023 (2004)